Terahertz superconducting plasmonic crystals

Zhen Tian (田 震)[1,2*], Jiaguang Han (韩家广)[1], Jianqiang Gu (谷建强)[1,2], Mingxia He (何明霞)[1], Qirong Xing (邢岐荣)[1], and Weili Zhang (张伟力)[1,2]**

[1]*Center for Terahertz Waves, College of Precision Instrument and Optoelectronics Engineering, Key Laboratory of Opto-electronics Information and Technical Science of Ministry of Education, Tianjin University, Tianjin 300072, China*

[2]*School of Electrical and Computer Engineering, Oklahoma State University, Stillwater, Oklahoma 74078, USA*

[*]*Corresponding author: tianzhen@tju.edu.cn;* [**]*corresponding author: jiaghan@tju.edu.cn*

Received December 9, 2010; accepted January 28, 2011; posted online June 29, 2011

We present a thermal active control over terahertz (THz) extraordinary transmission induced by a plasmon in a periodic subwavelength holes array and a patch array. Both arrays consist of high transition temperature YBCO superconductors using THz time domain spectroscopy (THz-TDS). In the periodic subwavelength YBCO holes array, we observe a transition between a virtual excitation type surface plasmon polaritons (SPP) mode and a real SPP mode accompanied with transmission amplitude modulation. This can be attributed to the *c*-axis Josephson plasma frequency. On the other hand, since dipole localized surface plasmon can be excited by direct optical illuminations without phase-matching techniques, we observe a transmission amplitude modulation induced by combining the normal state carriers and the superconducting carriers in the periodic subwavelength YBCO patch array. These THz superconducting plasmonic crystals hold great potential in application for extreme low-loss, large dynamic amplitude modulation, surface plasmon-based function devices.

OCIS codes: 300.6495, 240.6680.
doi: 10.3788/COL201109.S10403.

Over the past few years, research on extraordinary transmission of light through gratings of subwavelength holes in the field of surface plasmon optics (plasmonics) has gained increasing interest from both a scientific and a practical point of view[1−3]. Plasmonics has been regarded as a candidate technology for the production of next generation chips[4]. To realize the potential, however, a great challenge in the field of plasmonics is the active control of surface plasmon polaritons (SPPs). SPP-assisted light propagation can be controlled actively through thermal, optical, and electrochemical methods in the visible and near-infrared frequency regimes[5−7]. At terahertz (THz) frequencies, semiconductors are efficient materials for active plasmonics. Through carrier injection, temperature control or optical excitation, the density of free carriers in semiconductors can be modified actively. Thermal, electronic, magnetic, and optical switching of THz SPPs has been extensively demonstrated in recent years, allowing active control of SPP resonance[8−16]. Apart from semiconductors, another candidate active material is high transition temperature superconductors at THz frequencies. This kind of superconductor is a highly anisotropic material and has multilayer superconducting Cu_2O planes with interlayer tunneling of Cooper pairs between them, which brings about the *c*-axis Josephson plasma resonance (JPR). The JPR usually lies in the microwave and THz range[17]. Several theoretical papers have predicted the existence of a surface wave in high transition temperature superconductors[18−20].

In this letter, we present thermal active control over THz extraordinary transmission induced by a plasmon in a periodic subwavelength holes array and a patch array. Both arrays consist of high transition temperature YBCO superconductors using THz time domain spectroscopy (THz-TDS). In the periodic subwavelength YBCO holes array, we observed a sharp transition between a virtual excitation type SPP mode and a real SPP mode accompanied by transmission amplitude modulation. In the periodic subwavelength YBCO patch array, we observed a sharp transmission amplitude modulation induced by a combination of the normal state carriers and the superconducting carriers.

The sample was made from a commercial (THEVA, Germany) 280-nm-thick YBCO film, which typically had an 86-K transition temperature and 2.3-MA/cm^2 critical current density grown on a 500-μm-thick sapphire substrate. Using conventional photolithographic[21,22] exposure, we patterned a 3-μm-thick negative photoresist NR7-3000P film into the hole and patch shape on the YBCO film as a protective layer. The sample was then wet-etched in 0.04% nitric acid to remove YBCO from other parts of the wafer that did not have the photoresist protection. Lift-off in pure acetone followed. In this letter, we fabricated two samples: a holes array and a patch array (see Fig. 1). The 65 × 50 (μm) rectangular YBCO holes and 50 × 25 (μm) rectangular YBCO patches had the same periodicity of 100 μm.

The measurements were performed from room temperature to 77 K in a standard THz-TDS system, which consisted of four parabolic mirrors in an 8-F confocal geometry, with a useful bandwidth of 0.2–2.6 THz, a 2-mm THz beam size at waist, and an amplitude signal-to-noise ratio (SNR) greater than 3000:1. The transmitter of the system was a GaAs photoconductive switch gated by femtosecond laser beam with a repetition rate of 88 MHz,

and the detector used was a ZnTe module[23]. We used a vacuum chamber with a liquid nitrogen container in tight contact with the sample so that effective cooling of the sample was possible. The transmission is defined as $\left|\tilde{t}(\omega)\right| = |E_{\rm out}(\omega)/E_{\rm in}(\omega)|$, where $E_{\rm out}(\omega)$ and $E_{\rm in}(\omega)$ are the frequency-dependent amplitudes of the THz pulses transmitted through the sample and reference, respectively.

The measured normalized transmission response of the YBCO holes array and patch array at temperatures 297, 183, 133, and 86 K are shown in Figs. 1(a) and (b), respectively. For the YBCO holes array, we observed two resonance modes at 0.85 and 1.16 THz, with peak amplitudes of 0.686 and 0.508, corresponding to the $[\pm1, 0]$ mode and $[\pm1, \pm1]$ mode of the surface wave, respectively. With temperature decrease, the two resonance modes showed a frequency blue shift with peak amplitude increase. At the critical temperature of 86 K, the $[\pm1, 0]$ resonance mode shifted to 0.88 THz, with a peak amplitude of 0.75. For the YBCO patch array, we observed a resonance minimum at 0.87 THz with a minimum amplitude value of 0.42 induced by dipole localized surface plasmon (DLSP). With temperature decrease, the resonance minimum had a frequency blue shift with minimum amplitude decrease. At the critical temperature of 86 K, the resonance minimum shifted to 0.89 THz with a minimum amplitude value of 0.31.

YBCO is an anisotropic crystal, and the anisotropic dielectric function along the *ab*-plane and *c* axis can be written as[17]

$$\varepsilon_{\rm c}(\omega) = \varepsilon^{\rm c}_{\infty}(1 - \frac{\omega^2_{\rm pc}}{\omega^2} + \frac{4\pi i\sigma_{\rm c}}{\varepsilon^{\rm c}_{\infty}\omega}), \quad (1)$$

$$\varepsilon_{\rm ab}(\omega) = \varepsilon^{\rm ab}_{\infty}(1 - \frac{\omega^2_{\rm pab}}{\omega^2}), \quad (2)$$

where $\omega_{\rm pc}$ and $\omega_{\rm pab}$ are out-of-plane and in-plane plasma frequencies, respectively. The plasma frequency along the *c* axis is also called Josephson plasma frequency, and it usually lies in the microwave and THz ranges. YBCO is superconducting below the critical temperature. The plasma frequency along the *ab* plane can be directly measured from the normal incidence transmission, and we found it was close to the near-infrared regime.

The surface polaritons dispersion relation in YBCO can be expressed as[24]

$$k^2 = \frac{\omega^2}{c^2}\varepsilon_{\rm s}\varepsilon_{\rm c}\frac{\varepsilon_{\rm ab} - \varepsilon_{\rm s}}{\varepsilon_{\rm ab}\varepsilon_{\rm c} - \varepsilon^2_{\rm s}}, \quad (3)$$

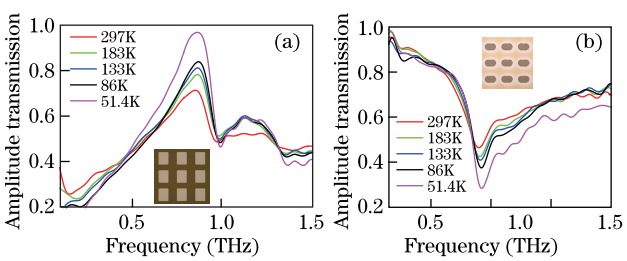

Fig. 1. (Color online) Measured normalized transmission response of YBCO (a) holes array and (b) patch array at normal incidence at 297, 183, 133, 86, and 51.4 K, respectively. The insets are the schematics of a periodic subwavelength YBCO holes array and a periodic subwavelength YBCO patch array, respectively.

where $\varepsilon_{\rm s}$ is the dielectric constant of the surrounding substrate. This dispersion relation is uniform with that in isotropic material if $\varepsilon_{\rm ab} = \varepsilon_{\rm c}$, from which we can obtain the dispersion relation in the isotropic material. For YBCO $\varepsilon_{\rm ab} \neq \varepsilon_{\rm c}$, there are two cases. When the temperature is lower than the critical temperature of 86 K, there are $\varepsilon_{ab} < 0$, $\varepsilon_c < 0$, and $|\varepsilon_{ab}| >> |\varepsilon_c|$. The dispersion relation can be simplified as $k^2 = \omega^2/c^2 \times \varepsilon_{\rm s}$. In this case, the THz wave can be coupled to a real SPP mode similar with the case in metal. When the temperature is higher than the critical temperature of 86 K, there are $\varepsilon_{ab} < 0$, $\varepsilon_c > 0$, and $|\varepsilon_{ab}| >> |\varepsilon_c|$. The dispersion relation can also be simplified as $k^2 = \omega^2/c^2 \times \varepsilon_{\rm s}$. Although the two types of cases have the same dispersion relation at the THz range, the surface mode is a virtual excitation type SPP for the second case, which only occurs at a small wave vector. Furthermore, virtual excitation type SPP must always be driven by the associated electromagnetic wave. When the associated electromagnetic wave is removed, the virtual excitation type SPP disappears at the same time[25]. From Fig. 1, we know that the transmission resonances are all caused by the virtual excitation type SPP above 86 K.

Moreover, we discuss the conductivity of YBCO above and below the critical temperature. Above critical temperature, the normal carriers determine the conductivity described by the Drude model. When the temperature varies from room to critical temperature, the conductivity slowly increases due to the decrease of collision frequency[23]. Above 86 K, the real part of conductivity dominates since the value of real conductivity is three orders of magnitude larger than the imaginary part. Below the critical temperature, the superconducting carriers behave according to the London equation. The total conductivity is then given as a sum of the normal and superconducting components, although the superconducting carriers contribute only to the imaginary part of the whole conductivity[26]. When the temperature of the experiment is reduced below the critical temperature, the imaginary part of the conductivity increases and finally exceeds the real part. In the THz regime, non-transition metals almost had a small ratio of real to imaginary dielectric constant ($-\varepsilon_r/\varepsilon_i << 1$). In this letter, a large ratio of real to imaginary dielectric constant at THz frequencies is preferred for high transition temperature superconductors, giving it potential for application in low-loss, large dynamic amplitude modulation, surface plasmon-based devices.

Due to material imperfections, such as cracks, voids or secondary phases, we were unable to observe a sharp change at 86 K. Using the measured real conductivity at 297, 183, 133, and 86 K, and the complex conductivity from literature at 51.5 K[27,28], we carried out a simulation of THz transmission of the periodic subwavelength YBCO holes array and a patch YBCO array using CST microwave studio (see Fig. 2). For the holes array, the transmission peak amplitude caused by the virtual excitation type SPP gradually became larger due to the increase of ratio of real to imaginary dielectric constant[29]. At the superconducting state, the transmission peak caused by a real SPP nearly reached 1 with extreme low loss. The frequency blue shift was caused by the increase of real part dielectric function[13]. For the

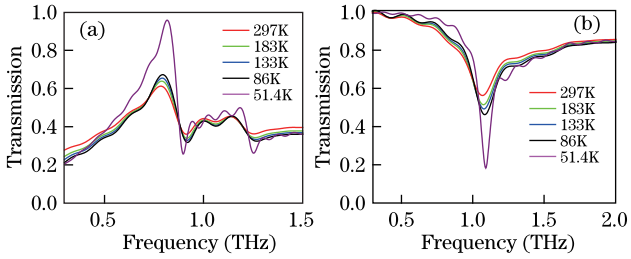

Fig. 2. Simulation of THz transmission of (a) a periodic subwavelength YBCO holes array and (b) a patch YBCO array using CST microwave studio.

patch array[30], due to the increase of conductivity, the transmission minimum amplitude became smaller and at the superconducting state, the transmission minimum sharply decreased dip. The frequency blue shift may be caused by patch size change due to skin depth change.

In conclusion, thermal active control over THz extraordinary transmission induced by a plasmon in a periodic subwavelength YBCO holes array and a patch YBCO array has been achieved. Sharp amplitude changes, both in the holes array and patch array, have also been observed. These THz superconducting plasmonic crystals hold potential for applications in low-loss, large dynamic amplitude modulation, surface plasmon-based devices.

This work was partly supported by the U.S. National Science Foundation, the National Key Basic Research Foundation of China (Nos. 2007CB310403 and 2007CB310408), the National Natural Science Foundation of China (Nos. 60578037 and 61007034), and the Tianjin Sci-Tech Programs (Nos. 08ZCKFZC28000 and 07ZCGHHZ01100).

References

1. T. W. Ebbesen, H. J. Lezec, H. F. Ghaemi, T. Thio, and P. A. Wolff, Nature **391,** 667 (1998).
2. W. L. Barnes, A. Dereux, and T. W. Ebbesen, Nature **424,** 824 (2003).
3. E. Ozba, Science **311,** 189 (2006).
4. R. Zia, J. A. Schuller, A. Chandran, and M. L. Brongersma, Material Today **9,** 20 (2006).
5. T. Nikolajsen, K. Leosson, and S. I. Bozhevolnyi, Appl. Phys. Lett. **85,** 5833 (2004).
6. S. Park and S. H. Song, Electron. Lett. **42,** 402 (2006).
7. Y. R. Leroux, J. C. Lacroix, K. I. Chane-Ching, C. Fave, N. Félidj, G. Lévi, J. Aubard, J. R. Krenn, and A. Hohenau, J. Am. Chem. Soc. **127,** 16022 (2005).
8. J. G. Rivas, P. H. Bolivar, and H. Kurz, Opt. Lett. **29,** 1680 (2004).
9. H. Chen, H. Lu, A. K. Azad, R. D. Averitt, A. C. Gossard, S. A. Trugman, J. F. O'Hara, and A. J. Taylor, Opt. Express **16,** 7641 (2008).
10. J. Han, A. Lakhtakia, Z. Tian, X. Lu, and W. Zhang, Opt. Lett. **34,** 1465 (2009).
11. J. G. Rivas, J. A. Sánchez-Gil, M. Kuttge, P. H. Bolivar, and H. Kurz, Phys. Rev. B **74,** 245324 (2006).
12. E. Hendry, M. J. Lockyear, J. G. Rivas, L. Kuipers, and M. Bonn, Phys. Rev. B **75,** 235305 (2007).
13. C. Janke, J. G. Rivas, P. H. Bolivar, and H. Kurz, Opt. Lett. **30,** 2357 (2005).
14. W. Zhang, A. K. Azad, J. Han, J. Xu, J. Chen, and X.-C. Zhang, Phys. Rev. Lett. **98,** 183901 (2007).
15. E. Hendry, F. J. G. Vidal, L. M. Moreno, J. G. Rivas, M. Bonn, A. P. Hibbins, and M. J. Lockyear, Phys. Rev. Lett. **100,** 123901 (2008).
16. A. K. Azad, H. Chen, S. R. Kasarla, A. J. Taylor, Z. Tian, X. Lu, W. Zhang, H. Lu, A. C. Gossard, and J. F. O'Hara, Appl. Phys. Lett. **95,** 011105 (2009).
17. V. K. Thorsmølle, R. D. Averitt, M. P. Maley, L. N. Bulaevskii, C. Helm, and A. J. Taylor, Opt. Lett. **26,** 1292 (2001).
18. H. A. Fertig and S. D. Sarma, Phys. Rev. Lett. **65,** 1482 (1990).
19. O. Keller, J. Opt. Soc. Am. B **7,** 2229 (1990).
20. S. Savel'ev, V. Yampol'skii, and F. Nori, Phys. Rev. Lett. **95,** 187002 (2005).
21. D. Qu, D. Grischkowsky, and W. Zhang, Opt. Lett. **29,** 896 (2004).
22. A. K. Azad, Y. Zhao, and W. Zhang, Appl. Phys. Lett. **86,** 141102 (2005).
23. R. Singh, Z. Tian, J. Han, C. Rockstuhl, J. Gu, and W. Zhang, Appl. Phys. Lett. **96,** 071114 (2010).
24. A. Hartstein, E. Burstein, J. J. Brion, and R. F. Wallis, Surface Science **34,** 81 (1973).
25. A. Hartstein, E. Burstein, J. J. Brion, and R. F. Wallis, Solid State Commun. **12,** 1083 (1973).
26. F. London and H. London, Proc. Roy. Soc. A **149,** 71 (1935).
27. M. Khazan, "Time-domain terahertz spectroscopy and its application to the study of high-Tc superconductor thin films," Ph.D Thesis (University Hamburg., 2002).
28. I. Wilke, M. Khazan, C. Rieck, P. Kuzel, T. Kaiser, C. Jaekel, and H. Kurz, J. Appl. Phys. **87,** 2984 (2000).
29. A. K. Azad, Y. Zhao, W. Zhang, and M. He, Opt. Lett. **31,** 2637 (2006).
30. X. Lu, J. Han, and W. Zhang, Appl. Phys. Lett. **92,** 121103 (2008).